



Implications of dietary carbon incorporation in fish carbonates for the global carbon cycle

Amanda M. Oehlert ^{a,*}, Jazmin Garza ^a, Sandy Nixon ^b, LeeAnn Frank ^b, Erik J. Folkerts ^b, John D. Stieglitz ^b, Chaojin Lu ^a, Rachael M. Heuer ^b, Daniel D. Benetti ^b, Javier del Campo ^{b,c}, Fabian A. Gomez ^{d,e}, Martin Grosell ^b

^a Department of Marine Geosciences, Rosenstiel School of Marine, Atmospheric, and Earth Science, University of Miami, FL, United States of America

^b Department of Marine Biology and Ecology, Rosenstiel School of Marine, Atmospheric, and Earth Science, University of Miami, FL, United States of America

^c Institut de Biología Evolutiva (CSIC - Universitat Pompeu Fabra), Barcelona, Spain

^d Northern Gulf Institute, Mississippi State University, MS, United States of America

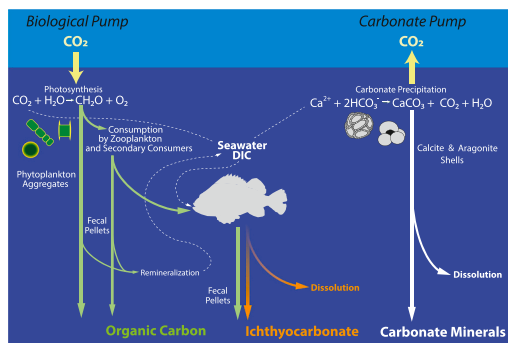
^e NOAA Atlantic Oceanographic and Meteorological Laboratory, Miami, FL, United States of America



HIGHLIGHTS

- Carbonate production by marine fish could be 2.7 to 9.5× greater than previously estimated.
- Assimilated dietary carbon comprises a significant fraction of ichthyocarbonate, ranging from 28 - 56 %, but up to 81 %.
- Organic matter in ichthyocarbonate may contribute an overlooked 0.08 to 1.61 Pg C yr⁻¹ to the biological pump.

GRAPHICAL ABSTRACT



ARTICLE INFO

Editor: Kuishuang Feng

Keywords:

Global carbon cycle
Marine fish
Osmoregulation
Biological pump
Carbonate pump
Stable carbon isotope ratios

ABSTRACT

Marine bony fish are important participants in Earth's carbon cycle through their contributions to the biological pump and the marine inorganic carbon cycle. However, uncertainties in the composition and magnitude of fish contributions preclude their integration into fully coupled carbon-climate models. Here, we consider recent upwards revisions to global fish biomass estimates (2.7–9.5 ×) and provide new stable carbon isotope measurements that show marine fish are prodigious producers of carbonate with unique composition. Assuming the median increase (4.17 ×) in fish biomass estimates is linearly reflected in fish carbonate (ichthyocarbonate) production rate, marine fish are estimated to produce between 1.43 and 3.99 Pg CaCO₃ yr⁻¹, but potentially as much as 9.03 Pg CaCO₃ yr⁻¹. Thus, marine fish carbonate production is equivalent to or potentially higher than contributions by coccolithophores or pelagic foraminifera. New stable carbon isotope analyses indicate that a significant proportion of ichthyocarbonate is derived from dietary carbon, rather than seawater dissolved inorganic carbon. Using a statistical mixing model to derive source contributions, we estimate ichthyocarbonate contains up to 81 % dietary carbon, with average compositions of 28–56 %, standing in contrast to contents <10

* Corresponding author.

E-mail address: aoehlert@miami.edu (A.M. Oehlert).

% in other biogenic carbonate minerals. Results also indicate ichthyocarbonate contains 5.5–40.4 % total organic carbon. When scaled to the median revised global production of ichthyocarbonate, an additional 0.08 to 1.61 Pg C yr⁻¹ can potentially be added to estimates of fish contributions to the biological pump, significantly increasing marine fish contributions to total surface carbon export. Our integration of geochemical and physiological analyses identifies an overlooked link between carbonate production and the biological pump. Since ichthyocarbonate production is anticipated to increase with climate change scenarios, due to ocean warming and acidification, these results emphasize the importance of quantitative understanding of the multifaceted role of marine fish in the global carbon cycle.

1. Introduction

Dynamics of the ocean's biological and carbonate pumps determine the concentration of atmospheric CO₂ over time periods less than a millennium (Buesseler et al., 2020; Elderfield, 2002; Frankignoulle et al., 1995; Honjo et al., 2014; Turner, 2015), making the production, composition, and export of organic matter and carbonate minerals a fundamental control on Earth's carbon cycle. The biological pump describes the export flux of photosynthetically fixed carbon and is responsible for the removal of dissolved CO₂ from the surface oceans (Buesseler et al., 2020; Nowicki et al., 2022) via gravitational sinking of phytoplankton aggregates, fecal pellets, and particle injection pumps (Boyd et al., 2019; Honjo et al., 2014; Nowicki et al., 2022; Pinti et al., 2023; Turner, 2015). The carbonate pump, on the other hand, refers to marine biogenic calcification which produces a sinking flux of carbonate minerals derived from dissolved inorganic carbon (DIC) in seawater that result in a net flux of CO₂ back to the atmosphere on time scales <1000 years (Elderfield, 2002; Frankignoulle et al., 1995). The balanced reaction for marine calcification indicates that every mole of carbonate precipitated should result in the release of one mole of CO₂ to surrounding seawater, however, *in situ* experiments showed that CO₂ release is moderated to ~0.6 mol by the buffering capacity of the oceans and concurrent photosynthetic uptake (Ware et al., 1991; Frankignoulle et al., 1994, 1995; Gattuso et al., 1993). Thus, through their concurrent impacts on DIC and alkalinity inventories in the ocean, the production of marine organic matter and carbonate minerals play a fundamental role in determining *p*CO₂ (Elderfield, 2002; DeVries, 2022; Nowicki et al., 2022).

Marine bony fish (teleosts) are important participants in the global carbon cycle, producing contributions to both the biological and carbonate pumps (Bianchi et al., 2021; Mariani et al., 2020; Pinti et al., 2023; Saba et al., 2021; Wilson et al., 2009; Woosley et al., 2012). Through prey consumption, fecal pellet production, diel vertical migration, and deadfall, marine fish contribute significantly to the biological pump (Bianchi et al., 2021; Mariani et al., 2020; Pinti et al., 2023; Saba et al., 2021). Marine bony fishes are also perpetual producers of carbonate precipitates (ichthyocarbonate) which form in their intestines as a result of their osmoregulatory strategy (Grosell et al., 2001), and are continuously excreted to the environment (Walsh et al., 1991; Wilson et al., 2009). Original production magnitude estimates based on global fish biomass between 0.81 and 2.05 Gt showed that ichthyocarbonate constituted 3–15 %, but plausibly up to 45 %, of global new carbonate production each year (Wilson et al., 2009), thus making ichthyocarbonate an important driver in the cycling of inorganic carbon in the world's oceans. Ichthyocarbonates are typically Mg²⁺ rich and composed of soluble minerals like high-magnesium calcite (HMC) and amorphous carbonate polymorphs (ACMC; Foran et al., 2013; Perry et al., 2011; Salter et al., 2019; Salter et al., 2018; Salter et al., 2012). The role of ichthyocarbonate in the carbonate pump is expected to be driven by production rate, composition, and characteristics like mineral solubility and sinking rate (Wilson et al., 2009; Woosley et al., 2012; Foran et al., 2013). While marine bony fishes have been intrinsically linked to multiple aspects of the global carbon cycle, uncertainty regarding the production magnitude and composition of their organic carbon and carbonate contributions currently limits their incorporation

into fully coupled climate-carbon earth system models (Bianchi et al., 2021; Mariani et al., 2020; Saba et al., 2021).

Ichthyocarbonate production and excretion is ubiquitous and central to physiological processes in all marine teleost fish studied thus far (Ghilardi et al., 2023; Grosell et al., 2001; Grosell and Oehlert, 2023; Perry et al., 2011; Perry et al., 2022; Salter et al., 2019; Salter et al., 2012; Wilson et al., 2009). Intestinal base secretion leading to the precipitation of ichthyocarbonate is essential for water balance in marine fish that drink seawater to stay hydrated (Grosell et al., 2001; Wilson et al., 2002; Grosell and Oehlert, 2023). Physiologists have long recognized that osmoregulation by marine fish requires an endogenous, and thus dietary, source of carbon to explain the high observed rates of total rectal base excretion (Shehadeh and Gordon, 1969; Walsh et al., 1991; Grosell and Genz, 2006). Drinking rates in marine fish are typically 2–5 mL kg⁻¹ h⁻¹, which equates to ingestion of 5–12 µ-equiv HCO₃ kg⁻¹ h⁻¹ (Grosell, 2010). By contrast, total rectal base excretions, including both HCO₃ ions and solid ichthyocarbonate precipitates, exceed 80 µ-equiv kg⁻¹ h⁻¹ (Grosell, 2010), indicating assimilated dietary carbon is required for at least 85 % of total rectal base excretions. Consequently, the predominant source of carbon for rectal base excretion originates from dietary carbon produced in the marine food-web, the base of which is supplied by photosynthetically-fixed carbon. However, a critical knowledge gap is whether assimilated dietary carbon is evenly partitioned between dissolved bicarbonate ions in intestinal fluid and the sinking flux of solid-phase ichthyocarbonates excreted by marine fish. If ichthyocarbonate is comprised of high concentrations of carbon derived from diet rather than seawater DIC, ichthyocarbonate precipitation may exert unexpected impacts on total alkalinity and DIC concentrations in the surface waters of the ocean when compared to other styles of marine calcification.

In this study, we aimed to update global estimates of ichthyocarbonate production using recent and substantial upwards revisions to estimates of global fish biomass (Bar-On et al., 2018; Bianchi et al., 2021; Irigoien et al., 2014; Jennings and Collingridge, 2015; Proud et al., 2017; Proud et al., 2018; Proud et al., 2019) and to evaluate the proportion of dietary carbon incorporated into solid-phase ichthyocarbonates. To test the hypothesis that significant proportions of carbon in ichthyocarbonate originate from fish diet, we conducted the first measurements of the stable carbon isotope values of the carbonate ($\delta^{13}\text{C}_{\text{ichthyo}}$) and organic fraction ($\delta^{13}\text{C}_{\text{org}}$) of ichthyocarbonate produced by four species of marine bony fish, including *Opsanus beta*, *Paralichthys olivaceus*, *Ocyurus chrysurus*, and *Rachycentron canadum*. We also assessed the total organic carbon content (TOC) of ichthyocarbonate, filling a key knowledge gap in the characterization of fish contributions to the biological and carbonate pumps (Saba et al., 2021). Our results suggest that the osmoregulation strategy of bony marine fish converts organic matter originating from primary production in the marine food web into a carbonate precipitate anticipated to sink rapidly through the water column. Thus, the production of ichthyocarbonate transforms carbon fixed by phytoplankton into a fast-sinking flux of carbonate minerals that can evade shallow remineralization, which hold overlooked implications for the role of marine fish in the global carbon cycle.

2. Materials and methods

2.1. Experimental animals

To study ichthyocarbonate produced by fish with varying metabolic rates, we selected four marine bony fish species that are locally convenient to obtain and maintain for these sampling efforts: Yellowtail snapper (Lutjanidae), Olive flounder (Paralichthyidae), Cobia (Rachycentridae), and Gulf toadfish (Batrachoidinae). Both the Gulf toadfish and Olive flounder exhibit benthic lifestyles, but live in tropical/subtropical and temperate settings respectively. Yellowtail snapper is a tropical to subtropical free swimming and active fish. Finally, Cobia is a fast-growing (Benetti et al., 2010, 2021), fast-swimming species inhabiting offshore and coastal tropical-temperate environments (Schaffer and Nakamura, 1989).

Yellowtail snapper, Olive flounder, and Cobia were reared at the University of Miami Experimental Hatchery (UMEH) facility on Virginia Key, Florida. The Yellowtail snapper utilized in the study were first generation (F1) progeny originating from wild broodstock fish collected in the coastal waters of the Atlantic Ocean off of Miami, Florida. The Olive flounder were progeny originating from a broodstock population of this species maintained at the UMEH facility where they spawn frequently, and juveniles are produced regularly (Geng et al., 2017; Stieglitz et al., 2021). Cobia were also reared at UMEH, where a breeding and research program encompassing all their life stages has been in place for over a decade (Benetti et al., 2008a, 2008b, 2010; Stieglitz et al., 2012). All individuals of these three fish species were reared and maintained in accordance with UM Institutional Animal Care and Use Committee (IACUC) approved practices (Protocols #20-138; #21-090), including feeding of a diet comprised of thawed and chopped natural prey items (squid and sardines) or a pelletized commercial marine grower diet (Skretting Europa). The fish rearing tanks used for maintaining the aforementioned species are flow-through Biscayne Bay seawater tanks at the UMEH facility. The tanks were supplied with filtered (1 μ m) and UV-sterilized seawater (salinity 34–36) under ambient temperature conditions (22–29 °C) for Yellowtail snapper and Cobia or chilled seawater conditions (18–24 °C) for Olive flounder.

Gulf toadfish were collected as bycatch from commercial bait shrimp trawlers operating out of Dinner Key, Miami, FL. Toadfish were treated with malachite green (0.05 mg/L malachite green and 15 mg/L formalin) weekly upon arrival at the Rosenstiel School of Marine, Atmospheric, and Earth Science and before experiments began to remove ectoparasites. Between 3 and 10 toadfish were kept in 60 L aerated aquaria supplied with flow-through Biscayne Bay seawater that was filtered (1 μ m) and UV-sterilized seawater (salinity 34–36) under ambient temperature conditions (22–29 °C). Toadfish were fed squid to satiation weekly. All experimental protocols conducted in aquaria at the Rosenstiel School were completed in accordance with the UM IACUC approved practices (Protocol #16-225).

2.2. Ichthyocarbonate collection and preparation

Samples of excreted ichthyocarbonate were collected from 60 L aquaria at the Rosenstiel School using disposable pipettes as previously (Perry et al., 2011; Woosley et al., 2012; Salter et al., 2012, 2014). Ichthyocarbonates collected from the UMEH rearing tanks were first collected using gentle siphoning of bottom water, and transfer of tank debris into a 15 L collection vessel (bucket). Following collection, the water in the vessel was swirled using a gentle stirring motion to concentrate ichthyocarbonate in a central location in the bottom, which was pipetted using transfer pipettes into centrifuge tubes. Centrifuge tubes containing ichthyocarbonates were transferred to an ISO Level 7 Clean room and processed in a Class 100 trace metal workstation. Ichthyocarbonates were rinsed briefly 3 times in ultrapure (18 MΩ) MilliQ water and dried in an oven at 35 °C overnight, and then stored in a desiccator prior to analysis. To test the impact of days since last meal on

$\delta^{13}\text{C}_{\text{ichthyo}}$ values and mol% MgCO_3 , samples of excreted ichthyocarbonate were collected in sequential days since prior feeding and prepared as described above. After collection, subsamples destined for stable carbon isotope analysis of the carbonate were transferred to 50 mL centrifuge tubes rinsed 3 times with MilliQ water, leached in 5 % H₂O₂ for 30 min, centrifuged, rinsed again with MilliQ water, and allowed to dry in an exhausted fume hood in the clean room. Two tailed *t*-tests assuming unequal variance were conducted on measurements of $\delta^{13}\text{C}$ values of H₂O₂ treated (*n* = 11) and untreated (*n* = 8) samples of ichthyocarbonate produced by the Gulf toadfish. Results indicated no statistical difference in sample pre-treatment for $\delta^{13}\text{C}$ values (*p* = 0.269). Subsamples collected for stable carbon isotope analysis of the organic matter and TOC content associated with the ichthyocarbonate were left untreated and dried in an oven at 40 °C overnight.

2.3. Carbonate $\delta^{13}\text{C}$ values and mol% MgCO_3

The $\delta^{13}\text{C}$ values of the ichthyocarbonate ($\delta^{13}\text{C}_{\text{ichthyo}}$) produced by four fish species (Gulf toadfish (*n* = 19), Yellowtail snapper (*n* = 3), and Olive Flounder (*n* = 2), and Cobia (*n* = 3)) were analyzed using previously described methods employing 100 % phosphoric acid digestion (Rosenheim et al., 2005) analyzed on an automated Kiel III attached to a Finnigan Delta Plus mass spectrometer housed in the Stable Isotope Laboratory at the University of Miami. Data are reported in the conventional notation and reported relative to Vienna Pee Dee Belemnite (V-PDB) and standardized relative to an internal standard calibrated to NBS-19 (National Bureau of Standards). Errors on these analyses were < 0.03 ‰ based on replicate analysis of laboratory standards.

Ichthyocarbonate produced by the Gulf toadfish was collected each day (*n* = 4) for a period of four days to evaluate whether days past last meal impacts $\delta^{13}\text{C}_{\text{ichthyo}}$ values and the mol% MgCO_3 content of ichthyocarbonate. After drying, samples were manually homogenized using an agate mortar and pestle. Corundum (Al₂O₃) was baked at 105 °C for 2–4 h to remove absorbed H₂O and then was added to each subsample analyzed for mol% MgCO_3 as an internal standard to allow for correction of *d*-spacing and 20 values. Analyses were conducted on a PANalytical X-Pert Pro (PANalytical Inc., Almelo, the Netherlands) X-ray Diffractometer (XRD). Sample scans were conducted between 23° and 72° 20, using a step interval of 0.01° and a count time of 1 s for each step. Following the example of a prior study calculating mol%Mg of ichthyocarbonate using XRD (Salter et al., 2019), we used the curve presented by Goldsmith et al. (1961) and assume all magnesium is present as MgCO₃.

Two-tailed *t*-tests assuming unequal variance of datasets were conducted in Microsoft Excel to determine whether $\delta^{13}\text{C}_{\text{ichthyo}}$ values and mol% MgCO_3 were statistically distinguishable between days past feeding, and *p* values were assessed at thresholds of 0.05 for significance.

2.4. Organic $\delta^{13}\text{C}$ values, %carbonate, and total organic carbon content

Dietary carbon sources were analyzed in triplicate for organic carbon isotope ($\delta^{13}\text{C}_{\text{org}}$) values, including squid, sardines, and a commercial pelletized diet (Skretting Europa). Triplicate samples of each diet were dried in an oven for 72 h at 40 °C and powdered prior to preparation for analysis. Dietary carbon samples and organic matter embedded within ichthyocarbonate produced by Gulf toadfish (*n* = 6), Olive Flounder (*n* = 6), and Yellowtail snapper (*n* = 3) were isolated for analysis via dissolution in 10 % HCl acid following methods described previously (Oehlert and Swart, 2014). Small sample sizes of ichthyocarbonate collected from Cobia unfortunately precluded analysis of TOC. To quantify the carbonate content of ichthyocarbonate, care was taken to collect ichthyocarbonate excreted independently of fecal pellets. Weight percent carbonate was calculated by mass loss after acid digestion (Oehlert and Swart, 2014). Samples were combusted using a Costech ECS 4010 (Costech Analytical Technologies, Inc., Valencia, CA, USA) and the resulting CO₂ gas was transferred for isotopic measurement to a continuous flow isotope-ratio mass spectrometer (Delta V Advantage,

Thermo Fisher Scientific, Waltham, MA, USA). The reproducibility of the measurements of stable carbon isotope values of the organic fraction ($\delta^{13}\text{C}_{\text{org}}$ values) was $\pm 0.1\text{‰}$ as indicated by the standard deviation of replicate analyses of internal standards of glycine ($n = 8$). All organic $\delta^{13}\text{C}$ values are reported relative to the Vienna Pee Dee Belemnite (V-PDB) scale, defined for organic carbon as the $\delta^{13}\text{C}$ value of graphite (USGS24) = -16.05‰ *versus* V-PDB (Coplen et al., 2006). Percentages of insoluble residue and TOC were calculated as mass proportions of total sample weight. The standard deviation of the TOC analyses was 0.4 % based upon repeated analyses of glycine ($n = 8$).

2.5. Stable carbon isotope mixing model

Proportional contributions of dietary carbon and seawater dissolved inorganic carbon to ichthyocarbonate composition were calculated using the mixing model IsoError (Phillips and Gregg, 2001) using single isotope and two sources executed in Microsoft Excel (<https://www.epa.gov/eco-research/stable-isotope-mixing-models-estimating-source-proportions>) accessed on October 23, 2023. IsoError is applicable to systems in which the number of sources does not exceed $n + 1$, where n is the number of isotope systems (Phillips and Gregg, 2001). In the teleost fish, two sources allow for the application of a single isotope systematic and the calculation of deterministic solutions incorporating errors associated with variation in the composition of the source materials, as well as mixture process errors (Hopkins and Ferguson, 2012). Required inputs to IsoError (Phillips and Gregg, 2001) include measurement replicates (n), the average (± 1 SD) source compositions, including seawater DIC (δB , sdB) and dietary carbon (δA , sdA) measured in this study, as well as the average (± 1 SD) $\delta^{13}\text{C}$ value of the ichthyocarbonate (δM , sdM).

We adapted a published two component mixing model previously used to quantify dietary carbon incorporation into teleost fish otoliths (Chung et al., 2019; Chung et al., 2020) to determine fractionation associated with ichthyocarbonate precipitation (Eq. (1)):

$$\delta^{13}C_{ICHTHYO} = C_{DIET} \times \delta^{13}C_{(HCO_3-DIET)} + C_{DIC} \times \delta^{13}C_{DIC} + \varepsilon \quad (1)$$

where C_{DIET} is the fraction of carbon derived from dietary carbon, C_{DIC} is the fraction of carbon from seawater DIC, (equivalent to $1-C_{DIET}$), and ε is the carbon isotope fractionation associated with carbonate formation (Chung et al., 2019; Chung et al., 2020; Fig. 1, Fig. S1).

For seawater $\delta^{13}\text{C}_{\text{DIC}}$ values, we considered three scenarios (Table S1) based on available published data for seawater from Biscayne Bay (−6 to +2 ‰; [Swart et al., 2013](#)) and mineralogical fractionation factors reported for HMC and dolomite ([Jimenez-Lopez et al., 2006](#); [Sheppard and Schwarzc, 1970](#)). In brief, to test the sensitivity of the mixing model to $\delta^{13}\text{C}_{\text{DIC}}$ values, we used minimum (−2.85 ‰), average (−2.17 ‰), and maximum $\delta^{13}\text{C}_{\text{DIC}}$ values (−1.5 ‰) from Biscayne Bay ([Swart et al., 2013](#)) representative of our sampling period. The $\delta^{13}\text{C}_{\text{diet}}$ composition for each species was measured in triplicate, with the ultimate $\delta^{13}\text{C}_{\text{diet}}$ value of the 50:50 mixture of squid and sardines fed to Cobia mathematically calculated. We considered the fractionation of $\delta^{13}\text{C}$ values of dietary carbon induced by (1) assimilation and CO_2 respiration (+1 ‰; [DeNiro and Epstein, 1978](#); [McConaughey et al., 1997](#)) and (2) hydration/hydroxylation of respired CO_2 to bicarbonate (+ ~ 9 ‰ at equilibrium ([Romanek et al., 1992](#))) to produce the $\delta^{13}\text{C}$ value of the intestinal bicarbonate in equilibrium with dietary carbon ($\delta^{13}\text{C}_{\text{HCO}_3\text{-DIET}}$, [Fig. 1](#), [Fig. S1](#)).

Mineralogical fractionation (ϵ) has not been defined for ichthyocarbonate, thus we also considered a range of ϵ based on mol% MgCO_3 content, including the fractionation for synthetic HMC containing as much as 13 mol% MgCO_3 (Jimenez-Lopez et al., 2006) and stoichiometric dolomite with 50 mol% MgCO_3 (Sheppard and Schwarcz, 1970). We use mol% MgCO_3 , based on previous measurements of ichthyocarbonate produced by the Gulf Toadfish (~50 %; Heuer et al., 2012) and yellowtail snapper (26–34 %; Salter et al., 2012). Mol% MgCO_3 for Cobia

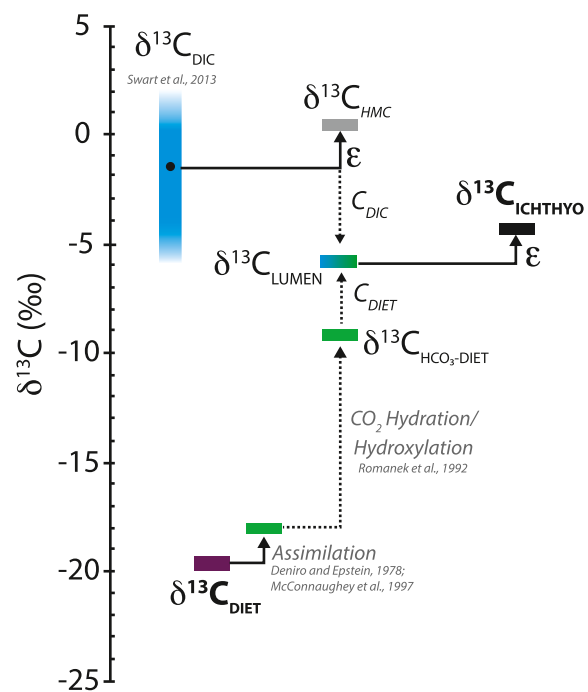


Fig. 1. Schematic representation of stable carbon isotope fractionation factors associated with ichthyocarbonate formation, including assimilation (DeNiro and Epstein, 1978; McConaughey et al., 1997), CO₂ hydration/hydroxylation (Romanek et al., 1992), and ϵ which represents the mineralogical fractionation between seawater and HMC that is based on mol%MgCO₃ content for HMC (Jimenez-Lopez et al., 2006) and dolomite (Sheppard and Schwarcz, 1970). The $\delta^{13}\text{C}$ value of the lumen results from mixing of bicarbonate from seawater DIC (C_{DIC}) and dietary carbon (C_{DIET}), the proportions of which impact the $\delta^{13}\text{C}$ value of ichthyocarbonate. Purple box shows the organic $\delta^{13}\text{C}$ value of the squid which was the food source used in measurements of specific dynamic action ('SDA') for the Gulf toadfish (Supplemental Fig. S2), and the black box represents the average carbonate $\delta^{13}\text{C}$ value of ichthyocarbonate measurements shown in Fig. 4.

and Olive flounder ichthyocarbonate are currently unknown, thus, we assumed the minimum and maximum values reported for Yellowtail Snapper (26–34 %; [Salter et al., 2012](#)) as conservative estimates (Table S1). Results from IsoError are reported as mean \pm 95 % confidence intervals on estimates of the contribution of carbon sources in ichthyocarbonate.

2.6. Accounting for updated estimates of global fish biomass

Initial quantification of global annual ichthyocarbonate production was based on global fish biomass estimates ranging between 0.812 and 2.05 Gt (Wilson et al., 2009). Since this seminal publication, updated global fish biomass estimates recognize a substantially larger global fish population, with biomass ranging between 0.9 and 19.5 Gt (Irigoien et al., 2014; Jennings and Collingridge, 2015; Proud et al., 2017, 2018, 2019; Bar-On et al., 2018; Bianchi et al., 2021). We calculated maximum relative increase factors of these papers compared to the maximum global fish biomass considered in 2009 by Wilson and colleagues (2.05 Gt). Variability in the increased estimates of global fish biomass appears to arise from technological approach and species focus. For instance, much of the increase in estimates of global fish biomass can be attributed to new methods of assessing mesopelagic fish biomass (Irigoien et al., 2014; Proud et al., 2017, 2018, 2019), while some global fish estimates are limited to specific latitudinal ranges (*i.e.*, Irigoien et al., 2014; Jennings and Collingridge, 2015; Proud et al., 2017), and size classes of fish (Bianchi et al., 2021).

Table 1

Compositional characteristics of diet fed to experimental fish. Average and standard deviation of the organic $\delta^{13}\text{C}$ values ($\delta^{13}\text{C}_{\text{org}}$) values of fish diets. *Indicates mathematical average of Squid 2 and Sardines fed to Cobia at the University of Miami Experimental Hatchery.

Species	n	Diet	$\delta^{13}\text{C}_{\text{org}}$ (‰ V-PDB)	St. dev. $\delta^{13}\text{C}_{\text{org}}$ (‰ V-PDB)
<i>Opsanus beta</i>	6	Squid 1	-19.6	0.7
<i>Paralichthys olivaceus, Ocyurus chrysurus</i>	3	Commercial diet (Skretting Europa)	-20.6	0.1
	-	50:50 mix Squid 2 and Sardines*	-20.2	0.6
<i>Rachycentron canadum</i>	3	Squid 2	-20.6	1.1
	3	Sardines	-19.7	0.1

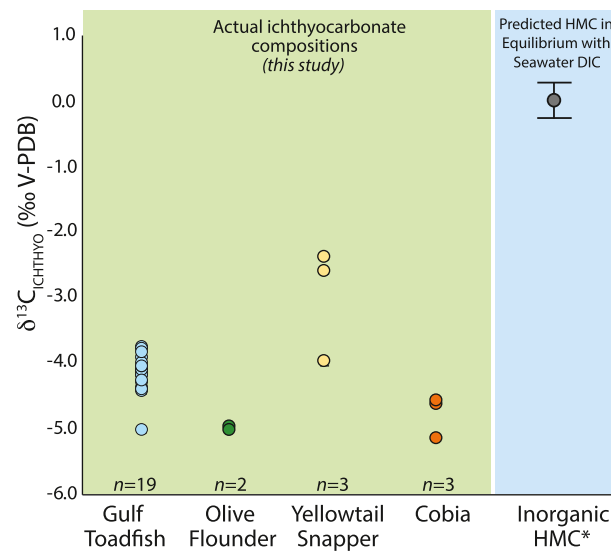


Fig. 2. Carbonate $\delta^{13}\text{C}$ values of ichthyocarbonates. Plot of carbonate $\delta^{13}\text{C}$ values of ichthyocarbonates (green shaded area of the plot) produced by the Gulf toadfish ($n = 19$), Olive Flounder ($n = 2$), Yellowtail Snapper ($n = 3$) and Cobia ($n = 3$). Standard deviations of replicate measurements of standards were $< 0.03 \text{ ‰}$, and error bars depicting standard deviation are smaller than the symbols representing individual measurements. The $\delta^{13}\text{C}$ value predicted for inorganic high-magnesium calcite (labeled Inorganic HMC*) assumes 50.5 mol% MgCO_3 to mimic concentrations in ichthyocarbonate produced by the Gulf toadfish. Using this mol% MgCO_3 composition, mineralogical fractionation was calculated from the equation defined by Jimenez-Lopez et al., 2006. Precipitation was assumed to occur in isotopic equilibrium with local seawater composition (from Swart et al., 2013) for the month of ichthyocarbonate sampling, and result is shown as a grey circle in the blue shaded area of the plot.

2.7. Estimating global ichthyocarbonate production and C_{DIET} incorporation

Using the minimum, maximum, median, and average reported increase in estimates of global fish biomass calculated above, we extrapolated these biomass increases linearly to the conservative initial estimates of ichthyocarbonate production (0.04 to 0.11 Pg $\text{CaCO}_3\text{-C yr}^{-1}$, Wilson et al., 2009) to evaluate the potential magnitude of updated ichthyocarbonate production. Using values of C_{DIET} assessed using IsoError, we also produced global estimates for dietary carbon incorporation rates, and calculate the total annual production in Pg $\text{CaCO}_3\text{-C}$ per year.

Table 2

Compositional characteristics of ichthyocarbonate produced by three species of marine fish. Average and standard deviation of percent total organic carbon content, percent carbonate content, particulate inorganic carbon to particulate organic carbon (PIC:POC), and organic $\delta^{13}\text{C}$ values ($\delta^{13}\text{C}_{\text{org}}$) values measured on ichthyocarbonate produced by the Gulf toadfish, Olive flounder, and Yellowtail snapper.

Species	n	%TOC (wt)	%Carbonate (wt)	PIC:POC	$\delta^{13}\text{C}_{\text{org}}$ (‰ V-PDB)
<i>Opsanus beta</i>	6	5.5 ± 2.4	86.5 ± 2.1	15.5	-19.2 ± 1.4
<i>Paralichthys olivaceus</i>	6	6.3 ± 1.6	86.5 ± 3.4	13.70	-21.2 ± 0.2
<i>Ocyurus chrysurus</i>	3	40.4 ± 6.6	24.5 ± 14.4	0.61	-23.8 ± 0.9

2.8. Estimating global annual production of ichthyocarbonate embedded TOC

Using %TOC measurements from ichthyocarbonate produced by the Gulf toadfish, Olive Flounder, and Yellowtail snapper coupled with the same estimates of global ichthyocarbonate production above, we calculated the minimum and maximum possible quantities of ichthyocarbonate-associated organic carbon in Pg C yr^{-1} and as a percent of the total carbonate production annually.

3. Results

3.1. Diet and ichthyocarbonate composition

Dietary carbon $\delta^{13}\text{C}_{\text{org}}$ values ranged from -20.6 to -19.6 ‰ V-PDB (Table 1). The $\delta^{13}\text{C}$ values of the carbonate mineral fraction of ichthyocarbonate produced by four marine bony fish species ranged from -5.16 to -2.41 ‰ with most samples characterized by $\delta^{13}\text{C}_{\text{ichthyo}}$ values lower than -3 ‰ (Fig. 2). On average, ichthyocarbonate produced by the Olive Flounder and Cobia exhibited the lowest $\delta^{13}\text{C}$ values, while ichthyocarbonate produced by the Yellowtail snapper exhibited the highest $\delta^{13}\text{C}$ values (Fig. 2). Stable carbon isotope measurements of ichthyocarbonate show that $\delta^{13}\text{C}_{\text{ichthyo}}$ values are depleted in ^{13}C relative to average DIC values from Swart et al. (2013), as well as the predicted $\delta^{13}\text{C}$ value of HMC precipitated in equilibrium with this DIC pool (Fig. 2) considering fractionation factors associated with HMC and stoichiometric dolomite (Jimenez-Lopez et al., 2006; Sheppard and Schwarcz, 1970).

The TOC content and $\delta^{13}\text{C}_{\text{org}}$ values of organic matter embedded in ichthyocarbonate were assessed on ichthyocarbonate produced by three marine fish species (Table 2). Ichthyocarbonate produced by Gulf toadfish ($n = 5$) contained on average $5.5 \pm 2.4 \text{ % TOC}$, Olive flounder ichthyocarbonate ($n = 3$) contained $6.3 \pm 1.6 \text{ %}$, and Yellowtail snapper ichthyocarbonate contained $40.4 \pm 6.6 \text{ %}$ (Table 2). Carbonate content averaged 65.7 % across the three species, with variability noted between species, and PIC:POC ratios ranged from 0.61 to 15.5 (Table 2).

Daily collection of ichthyocarbonate excreted by *Opsanus beta* allowed for assessment of changes in the $\delta^{13}\text{C}_{\text{ichthyo}}$ values and mol% MgCO_3 resulting from changes in metabolic rate induced by feeding state. No statistically significant differences were observed in either $\delta^{13}\text{C}_{\text{ichthyo}}$ values or mol% MgCO_3 of excreted ichthyocarbonate produced 1, 2, 3, or 4 days past last meal (Table 3, $p > 0.05$ for all comparisons).

Table 3

Measured $\delta^{13}\text{C}_{\text{ichthyo}}$ values and mol% MgCO_3 of ichthiocarbonate produced by the Gulf toadfish in successive days since last feeding. Results are reported as average \pm standard deviation, and sample number for both measurements of ichthiocarbonate, split by days since last meal.

Days since meal	n	Avg. $\delta^{13}\text{C}_{\text{ichthyo}}$ (‰V-PDB)	n	mol% MgCO_3
1	16	-3.12 ± 0.65	4	49.2 ± 0.5
2	14	-3.47 ± 0.37	4	49.3 ± 0.5
3	18	-2.81 ± 0.37	4	49.3 ± 0.4
4	22	-3.03 ± 0.68	4	49.1 ± 0.1

3.2. C_{DIET} in Ichthiocarbonate

IsoSource mixing model estimates of the proportion of C_{DIET} incorporated into ichthiocarbonate using our measurements of $\delta^{13}\text{C}_{\text{ichthyo}}$ values resulted in a mean range of dietary carbon incorporation between 21–36 %, 25–56 % and 43–69 % \pm 95 % confidence intervals (Fig. 3A-C) based on $\delta^{13}\text{C}_{\text{DIC}}$ values and ε assumed in each of the three scenarios evaluated (Fig. 2A-C; parameterization of IsoError reported in Table S1).

Using measured $\delta^{13}\text{C}_{\text{ichthyo}}$ values for each species (Fig. 2), our new measurements of $\delta^{13}\text{C}_{\text{diet}}$ (Table 2) and ε based on relationship published by Jimenez-Lopez et al. (2006) and Sheppard and Schwarcz (1970), our calculated mean C_{DIET} values range from 19 % for Yellowtail Snapper to 44 % for Cobia (Fig. 3A, Table S1 reports IsoError parameterization). Lower estimates are observed when minimum $\delta^{13}\text{C}_{\text{DIC}}$ and ε values are considered (Fig. 3B, Table S1). Estimates of C_{DIET} rise for all species when we assume ε values from Sheppard and Schwarcz (1970) and range from 41 % for Yellowtail Snapper to 64 % for Gulf Toadfish, with 95 % confidence intervals reaching as high as 81 % for toadfish ichthiocarbonate (Fig. 3C, Table S1).

3.3. Ichthiocarbonate-based global carbon fluxes

Maximum global fish biomass estimates since 2009 (Fig. 4) ranged between a factor of 0.98 to $9.51 \times$ higher than initially appreciated, with an average of $4.74 \times$ and median of $4.17 \times$ (Table 4). By linearly increasing conservative estimates of global ichthiocarbonate production rates (0.04 to 0.11 Pg $\text{CaCO}_3\text{-C yr}^{-1}$) quantified by Wilson et al. (2009) by the minimum, median, average, and maximum factors of

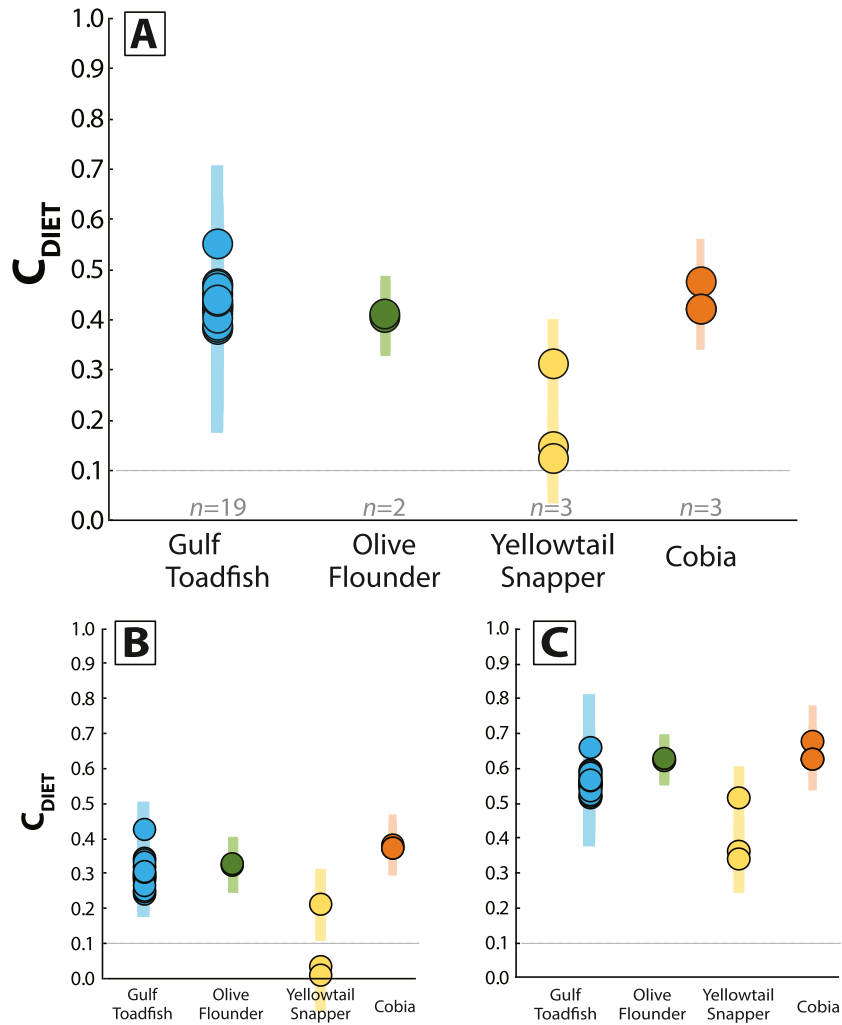


Fig. 3. Proportion of mean dietary carbon incorporation into ichthiocarbonates (C_{DIET} ; \pm 95 % confidence intervals) assessed for three scenarios using the IsoError mixing model. Results shown are mean C_{DIET} (circles) \pm 95 % confidence intervals (bars) predicted by calculations conducted using the IsoError mixing model (Phillips and Gregg, 2001) for each measurement of $\delta^{13}\text{C}_{\text{ICHTHYO}}$. The composition of the diet fed to each species is reported in Table 1 for all three scenarios. $\delta^{13}\text{C}_{\text{DIC}}$ values and ε were varied for each scenario (A-C) as follows: A) The $\delta^{13}\text{C}_{\text{DIC}}$ value = -2.85 ‰ , ε was assumed to be the minimum fractionation factor from Jimenez-Lopez et al. (2006), calculated from mol% MgCO_3 content for each species (Table S1). B) The $\delta^{13}\text{C}_{\text{DIC}}$ value = -2.17 ‰ (Swart et al., 2013), ε was assumed to be the average fractionation factor from Jimenez-Lopez et al. (2006), calculated from mol% MgCO_3 content for each species (Table S1). C) The $\delta^{13}\text{C}_{\text{DIC}}$ value = -1.5 ‰ (Swart et al., 2013), ε was assumed to be the fractionation factor reported by Sheppard and Schwarcz (1970) for dolomite with (Table S1). Note IsoError results for Yellowtail snapper in B exhibit negative values for confidence intervals.

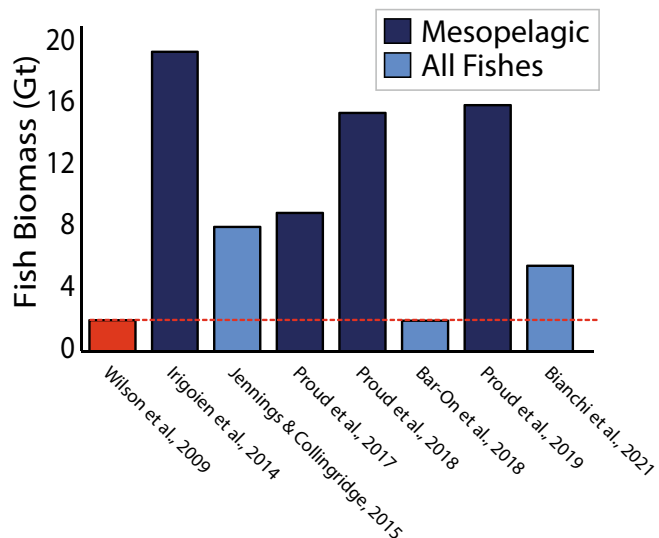


Fig. 4. Estimates of global fish biomass since 2009. Comparison of maximum estimates of global fish biomass in Gt published since 2009, when the upper estimate of 2.05 Gt fish biomass was used to calculate global ichthyocarbonate production (Wilson et al., 2009). Cited studies refer only to marine fish biomass with the exception of Bar-On et al., 2018, which considered the global biosphere.

Table 4

Calculation of increase factors for marine fish biomass. All studies refer to global marine fish biomass, with the exception of Bar-On et al., 2018.

Reference	Max biomass reported (Gt)	Factor
Wilson et al., 2009	2.05	1.00
Irigoen et al., 2014	19.5	9.51
Jennings and Collingridge, 2015	8.10	3.95
Proud et al., 2017	9.00	4.39
Proud et al., 2018	15.50	7.56
Bar-On et al., 2018	2.0	0.98
Proud et al., 2019	16.0	7.80
Bianchi et al., 2021 (Discounted by peak catch)	5.57	2.71
Minimum		0.98
Average		4.74
Median		4.17
Maximum		9.51

increase in global fish biomass estimates (Table 4), we estimate that marine fish may potentially produce between 0.33 and 9.03 Pg $\text{CaCO}_3 \text{ yr}^{-1}$ (Table 5). Since all marine bony fishes examined previously were shown to produce ichthyocarbonate (Grosell et al., 2001; Wilson et al., 2009), we also extrapolate potential ranges of C_{DIET} on a global scale. Considering our estimated potential range of ichthyocarbonate production, as well as calculated C_{DIET} values, between 0.09 and 5.05 Pg $\text{CaCO}_3 \text{ yr}^{-1}$ produced by marine fish are derived from dietary carbon,

with a median estimate between 0.40 and 2.23 Pg CaCO_3 annually (Table 5). Upscaling our measurements of %TOC in ichthyocarbonate produced by the Gulf toadfish, the Olive flounder, and the Yellowtail Snapper (Table 2) and our updated estimates of annual ichthyocarbonate production, we can estimate a potential range for the total annual production of ichthyocarbonate ballasted organic matter. When median increase in biomass estimates are considered, global annual production of ichthyocarbonate-associated organic matter may range between 0.08 and 1.61 Pg C yr^{-1} depending on the %TOC considered (Table 5).

4. Discussion

4.1. Dietary carbon incorporation into ichthyocarbonates

Our new measurements of $\delta^{13}\text{C}$ values of ichthyocarbonate produced by four bony fish species with varying lifestyles show that high rates of C_{DIET} incorporation are responsible for producing low $\delta^{13}\text{C}_{\text{ichthyo}}$ values (Figs. 1, 2). Thus, in contrast to other calcifiers, marine teleost fish rely little on DIC for carbonate production. Production and excretion of ichthyocarbonates is a ubiquitous process observed in all studied marine bony fish to date (Ghilardi et al., 2023; Grosell et al., 2001; Grosell and Oehlert, 2023; Perry et al., 2011; Perry et al., 2022; Salter et al., 2019; Salter et al., 2012; Wilson et al., 2009), thus we anticipate that similar trends for other species will arise with future study.

Besides incorporation of dietary carbon, we also considered the potential impacts of fractionation induced by pH and kinetic effects arising from metabolic rate on $\delta^{13}\text{C}_{\text{ichthyo}}$ values and mol% MgCO_3 . Carbon isotope partitioning resulting from increased pH in the intestinal lumen (8.4 to 9; McDonald and Grosell, 2006; Wilson et al., 2002) relative to seawater would be expected to produce higher, and not lower $\delta^{13}\text{C}_{\text{ichthyo}}$ values (Zeebe and Wolf-Gladrow, 2001). Kinetic effects, including discrimination against ^{13}C during CO_2 hydration and hydroxylation or changes in calcification rates (McConaughey, 1989), do not appear to exert a significant control since ichthyocarbonate collected daily does not exhibit significant differences in $\delta^{13}\text{C}_{\text{ichthyo}}$ values or mol% MgCO_3 with time since last feeding (Table 3), although this data was gathered only for crystalline phases of ichthyocarbonate produced by a single species. Metabolic rate is positively correlated with quantity of food consumed (Jobling and Davies, 1980), with peak metabolic rate occurring <12 h post feeding in most fish species (Jobling, 1981). Since ichthyocarbonate production rate is correlated with metabolic rate (Ghilardi et al., 2023; Grosell et al., 2001; Grosell and Oehlert, 2023; Perry et al., 2011; Perry et al., 2022; Salter et al., 2019; Salter et al., 2012; Wilson et al., 2009) and SDA measurements conducted on the Gulf toadfish indicate peak metabolic rate 3–4 h post feeding (Fig. S2), evidence of kinetic isotope fractionation driven by metabolic rate, expressed as lower $\delta^{13}\text{C}_{\text{ichthyo}}$ values, should be expected for ichthyocarbonate collected on the first day after feeding. However, no significant differences were observed in $\delta^{13}\text{C}_{\text{ichthyo}}$ values or mol% MgCO_3 of excreted ichthyocarbonate produced 1, 2, 3, or 4 days past last fish meal (Table 2, $p > 0.05$ for all comparisons), providing additional support for the interpretation that variations in the incorporation of metabolic CO_2

Table 5

Revised global estimates of ichthyocarbonate production, ichthyocarbonate derived from C_{DIET} , and ichthyocarbonate-associated organic matter. Assumptions for each calculation are listed in italics, increase factors are average, median, and maximum from Table 4. Increase factors for global fish biomass are synthesized in Table 4 based on literature review, and bolded row (4.17 \times) represents the median increase factor.

Biomass increase factors	Ichthyocarbonate production Pg $\text{CaCO}_3 \text{ yr}^{-1}$	Ichthyocarbonate from dietary carbon Pg $\text{CaCO}_3 \text{ yr}^{-1}$	Embedded organic matter Pg C yr^{-1}
$C_{DIET} / \% \text{TOC}$ $\text{Pg } \text{CaCO}_3 \text{ yr}^{-1}$	— 0.33	— 0.93	28 % 0.33
1.00 \times (no change)	0.33	0.93	56 % 0.95
4.17 \times	1.43	3.99	5.5 % 0.33
4.74 \times	1.60	4.47	40.4 % 0.95
9.51 \times	3.23	9.03	0.02 0.38
			0.08 1.61
			0.09 1.80
			0.18 3.64

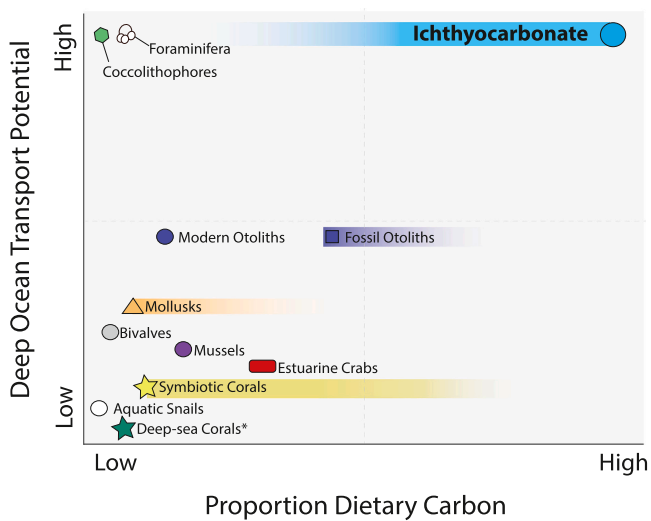


Fig. 5. Range of metabolic CO_2 incorporation and deep-ocean transport potential for marine calcifiers. Conceptual model linking the ratio of dietary carbon, as metabolic CO_2 , to seawater-derived carbon and the deep-ocean transport potential of calcium carbonate producers. Range of dietary carbon incorporation for ichthyocarbonate is based on the results of this study, while studies estimating the proportion of dietary carbonate incorporation for other biogenic carbonate producers shown here are listed in Table S2. The blue bar and circle representing ichthyocarbonate metabolic CO_2 shows the range of possible incorporation rates based on IsoError results presented in Fig. 3A-C, and results of physiological mass balance indicating 89.6–95.6 % (Genz et al., 2008; Heuer et al., 2012; Wilson et al., 1996a, 1996b).

are responsible for the disequilibrium $\delta^{13}\text{C}_{\text{ichthyo}}$ values observed in this study. Importantly, this interpretation is also independently supported by physiological mass balance of drinking and total rectal base excretion rates indicating that seawater DIC ingested during drinking is insufficient to supply total rectal base excretion rates (Genz et al., 2008; Heuer et al., 2012; Heuer et al., 2016; Wilson et al., 1996a, 1996b).

With better understanding of carbon isotope fractionation induced by biological processes, estimates of dietary carbon incorporation into ichthyocarbonates may result in improved agreement with physiological measurements. Ichthyocarbonate produced by different species is indeed characterized by wide ranging mol% MgCO_3 contents (Salter et al., 2017, 2018, 2019), but mineralogy appears to be largely controlled by family differences and relative intestinal length (Ghilardi et al., 2023), a relationship that should be investigated further. Another possible area of variability could include the repeated hydration of CO_2 to produce HCO_3^- , a process mediated by carbonic anhydrase, with anion exchangers and co-transporters transporting HCO_3^- across the intestinal epithelium (Fig. 2; Grosell and Genz, 2008; Genz et al., 2011). We anticipate that fractionations induced by enzymatic processes and selective HCO_3^- transporters may also impact the $\delta^{13}\text{C}$ values of bicarbonate available in the intestinal lumen for incorporation into ichthyocarbonates. Consequently, these observations highlight the need for controlled experiments to define fractionation factors relevant to the physiology of marine fish. Nevertheless, general agreement between our isotopic mass balance approach and physiological measurements indicates that significantly high proportions of dietary carbon are incorporated into the sinking flux of ichthyocarbonates (Fig. 5, Table S2) relative to other biogenic carbonate minerals.

4.2. Global production rates of ichthyocarbonate and embedded organic matter

Our new estimates of global ichthyocarbonate production rate, which take into account recently recognized increases in estimates of global fish biomass (Bar-On et al., 2018; Bianchi et al., 2021; Irigoien

et al., 2014; Jennings and Collingridge, 2015; Proud et al., 2017; Proud et al., 2018; Proud et al., 2019), indicate that the contribution of marine fish to the inorganic carbon cycle may have been significantly underestimated previously. Linear extrapolation of ichthyocarbonate production defined previously (Wilson et al., 2009) by factors proportional to recently recognized fish biomass (Table 4), suggests that marine bony fish may produce between 0.33 and 9.03 Pg CaCO_3 yr^{-1} (Table 5) or 0.04 to 1.08 Pg $\text{CaCO}_3\text{-C}$ yr^{-1} . Compared to annual new carbonate production by other marine calcifiers, our updated estimates suggest carbonate production by marine fish approaches or even exceeds that of pelagic foraminifera ($\sim 1.0\text{--}1.2$ Pg $\text{CaCO}_3\text{-C}$ yr^{-1} ; (Langer, 2008)), coccolithophores ($\sim 1.0\text{--}1.2$ Pg $\text{CaCO}_3\text{-C}$ yr^{-1} ; (Broecker and Clark, 2009; Godrijn et al., 2022)) as well as coral reefs (0.108 Pg $\text{CaCO}_3\text{-C}$ yr^{-1} ; (Iglesias-Rodriguez et al., 2002; Milliman and Droxler, 1996)). Our estimates also suggest that carbonate production by marine fish may even exceed some estimates of total new carbonate production in the oceans each year (0.5 and 2 Pg $\text{CaCO}_3\text{-C}$ yr^{-1} (Iglesias-Rodriguez et al., 2002; Milliman and Droxler, 1996)). Interestingly, a recent study by Buitenhuis et al. (2019) estimated that global production of aragonite by pteropods also exceeded total oceanic carbonate production (4.2 Pg $\text{CaCO}_3\text{-C}$ yr^{-1}) but suggested that a significant fraction of pteropod aragonite likely dissolved at relatively shallow depths in the water column. It is plausible that the same hypothesis applies to ichthyocarbonate as well, which is more likely to be soluble than aragonite (Woosley et al., 2012) as a result of high mol% MgCO_3 contents and ACMC phases (Foran et al., 2013; Perry et al., 2011; Salter, 2013; Salter et al., 2017; Salter et al., 2019; Salter et al., 2018; Salter et al., 2012; Salter et al., 2014; Walsh et al., 1991; Wilson et al., 2009).

In addition to carbonate mineral content, ichthyocarbonates also contain embedded organic matter, likely derived from their proteinaceous matrix and not undigested particles of food (Schauer et al., 2018a; Schauer and Grosell, 2017; Schauer et al., 2016; Schauer et al., 2018b), the abundance of which we define here for the first time (Table 1). Upscaling our measurements of %TOC using updated ichthyocarbonate production rate estimates indicates that ichthyocarbonate-associated organic matter may range between 0.08 and 1.61 Pg C yr^{-1} (Table 5). Our average and median estimates of ichthyocarbonate-associated organic matter (Table 5) suggests that fish-produced contributions to the biological pump (*i.e.*, $1.5\text{--}1.2$ Pg C yr^{-1} , estimated to be $\sim 16\%$ of total biological pump contributions (Saba et al., 2021)) are likely increased by ichthyocarbonate-associated organic matter. In addition, our results indicate a wide variation in the particulate inorganic carbon to particulate organic carbon (PIC:POC) ratio of ichthyocarbonates, ranging from 0.61 to 15.5, the high end of which is nearly an order of magnitude higher than coccolithophores (Findlay et al., 2011). Thus, ichthyocarbonate is predicted to act like a ‘time-release capsule’ for embedded organic matter, preventing remineralization in the shallow ocean and increasing sinking rates (‘ballast effect’ (Armstrong et al., 2002)). For example, sinking rates of POC associated with calcite (2.71 g cm^{-3}) may be variable (Gloege et al., 2017), but are thought to be $\sim 50\%$ faster with lower rates of respiration than aggregates of an equivalent size ballasted with siliceous diatoms (2.1 g cm^{-3}) (Klaas and Archer, 2002). Further, in comparison to the density of fecal pellets produced by copepods and macrozooplankters ($1.09\text{--}1.24\text{ g cm}^{-3}$) (Urban et al., 1993; White et al., 2018), sinking fluxes associated with carbonate minerals like ichthyocarbonate are anticipated to be faster (Armstrong et al., 2002). Thus, ichthyocarbonate is proposed to be an efficient mineral-ballasted carbon export mechanism. Consequently, the embedded organic matter in the ichthyocarbonate flux is likely to experience higher sequestration potential than other particulate organic matter, like fecal pellets. Incorporation of ichthyocarbonate into fecal pellets (*i.e.*, Perry et al., 2011; Salter et al., 2012, 2014; Saba et al., 2021) may also augment fecal pellet sinking rates due to higher density of mineral precipitates incorporated into the organic matter.

Of the total organic carbon export from the surface ocean, the current view is that most ($>90\%$) is consumed, respired, and recycled within

the mesopelagic depths of the ocean (Weber et al., 2016) and only a small fraction (<1–10 %) reaches the deep ocean for sequestration on the scales greater than millennia (Buesseler et al., 2020; Honjo et al., 2014; Turner, 2015). Fish fecal pellets have been observed to sink as quickly as 1000 m per day (Saba et al., 2021; Saba and Steinberg, 2012; Staresinic et al., 1983), limiting rates of remineralization in the shallow ocean. Such fast sinking rates have been suggested to increase the importance of the fish fecal pellet flux with depth (Bianchi et al., 2021; Saba et al., 2021). Indeed, at carbon sequestration relevant depths of 1000 m, fish fecal pellets have been estimated to increase in importance and constitute ~10 % of the global sinking particle flux because of differential sinking rates originating from by particulate matter source and composition (Bianchi et al., 2021). We argue that the five-fold increase in importance of fish fecal pellets at 1000 m relative to 200 m (Bianchi et al., 2021) may be extended to ichthyocarbonates, because they are also expected to sink rapidly.

4.3. Implications of anomalous dietary carbon incorporation

Accounting for our expected range in C_{DIET} (Table S1), we estimate that between 0.09 and 5.05 Pg $\text{CaCO}_3 \text{ yr}^{-1}$ (Table 5) is derived from the marine food web, rather than seawater DIC. Incorporation of significant quantities of dietary carbon into ichthyocarbonate makes intestinal calcification by bony fish anomalous with respect to other marine calcifiers, which typically contain <10 % on average (Fig. 5, Table S2). Unlike the skeletons and shells comprising the carbonate pump, which are a net source of CO_2 to the atmosphere during their formation (Frankignoulle et al., 1994; Frankignoulle et al., 1995), the fact that ichthyocarbonate is comprised of substantial quantities of metabolic CO_2 rather than seawater DIC may provide an overlooked connection between the carbonate and biological pumps. Such a connection would be based on the osmoregulation strategy of marine fish, a process that converts atmospheric CO_2 fixed by marine photosynthesis to a sinking flux of carbonate minerals and organic matter. A similar connection was recently proposed for coccolithophores, but their metabolic CO_2 incorporation occurs at significantly lower rates (~1.3 %, (Godrijan et al., 2022)) than estimated for ichthyocarbonate produced by marine fish (average of 28–56 %, but up to 81 %, Fig. 3).

By incorporating high quantities of assimilated dietary carbon into rapidly sinking carbonate precipitates with embedded organic matter, ichthyocarbonate acts like a mineralized counterpart to the conversion of phytoplankton into more resistant biomass and sinking fecal pellets. The fact that ichthyocarbonates are also likely to have high sinking rates physically separates total rectal base excretions, including solid ichthyocarbonate and bicarbonate ions, from the H^+ excretion occurring at the gill (Wilson et al., 2009). Protons arising from hydration reactions in the intestinal tissue are secreted to the blood (Grosell and Genz, 2006) and excreted by the gills (Genz et al., 2008; Fig. 2). Because of this anatomical separation of H^+ excretion from total rectal base excretion (Wilson et al., 2009), further measurement of the net acid-base balance of marine fish is warranted. Published estimates suggest net excretion of acid-base equivalents by marine fish is neutral (Perry et al., 2010) or slightly acidic (Genz et al., 2008), and future work should quantify whether complete dissolution of excreted ichthyocarbonates is needed to balance acid secretion at the gills, especially in the context of diurnal fish migration (Saba et al., 2021; Pinti et al., 2023). The deep-ocean transport potential of ichthyocarbonate, which impacts the fate and impact of marine carbonates on the global carbon cycle, is likely higher than other carbonate producers with sessile lifestyles (Fig. 5). Given their rapid production rates, high concentration of diet-derived carbon relative to other marine calcifiers (Figs. 3, 5), and likely high sinking rates, quantitative parameterization of the ichthyocarbonate export flux is an important next step in including marine fish into global biogeochemical models. Notably, mesopelagic fish constitute a significant proportion of marine fish biomass (Irigoien et al., 2014; Proud et al., 2019) and their lifestyle may give ichthyocarbonates a ‘head start’

towards depths where carbon is sequestered for >100 years (Saba et al., 2021; Pinti et al., 2023).

Although marine fish incorporate dietary carbon into ichthyocarbonate at anomalous rates compared to other marine carbonates, high overall production rates by other calcifying organisms (Broecker and Clark, 2009; Buitenhuis et al., 2019; Iglesias-Rodriguez et al., 2002; Langer, 2008; Milliman and Droxler, 1996) suggests that a significant proportion of marine carbonate produced by other calcifiers may also not conform to the paradigm of marine calcification and CO_2 emissions (Fig. 6). When the total carbonate produced annually by coccolithophores, foraminifera, marine fish, pteropods, and coral reefs (Broecker and Clark, 2009; Buitenhuis et al., 2019; Iglesias-Rodriguez et al., 2002; Langer, 2008; Milliman and Droxler, 1996; Wilson et al., 2009; this study) is corrected for the fraction of metabolic carbon incorporation (Godrijan et al., 2022; McConaughey, 1989; McConaughey et al., 1997; Spero and Lea, 1996; Wilson et al., 1996a, 1996b; this study), marine fish are revealed to be the most important contributor of carbonate originating from dietary carbon in the oceans today. Pelagic foraminifera, which produce ~1–1.2 Pg $\text{CaCO}_3\text{-C yr}^{-1}$ (Langer, 2008) with lower incorporation rates of metabolic CO_2 (<12 %, (Spero and Lea, 1996) are another important producer of carbonate derived from assimilated dietary carbon. Dietary carbon incorporation into aragonite produced by pteropods is currently unknown, but data from six species indicates they are ^{13}C -depleted relative to expected equilibrium aragonite (Grossman et al., 1986), suggesting that dietary carbon is likely incorporated into pteropod tests. Future studies should consider quantifying dietary carbon incorporation by pteropods, especially since they may be produced in high abundance but dissolve at shallow depths (Buitenhuis et al., 2019). Considering the upper end of production and dietary carbon incorporation for all major calcifiers (Godrijan et al., 2022; Heuer et al., 2012; McConaughey, 1989; McConaughey et al., 1997; Spero and Lea, 1996; Wilson et al., 1996a, 1996b; this study), it is possible that significantly more carbonate is produced each year than previously appreciated, and further, a significant proportion of total new marine carbonate production each year may be derived from dietary carbon. Such observations motivate future research elucidating the incorporation of metabolic CO_2 during marine calcification and its impacts on surface ocean carbonate chemistry in order to better understand the oceans' response to changes in the global carbon cycle.

4.4. Uncertainty and caveats

Revised global annual production rates of ichthyocarbonate, carbonate derived from dietary carbon, and new estimates of the embedded organic matter represent a first order re-evaluation of the role of marine fish in the global carbon cycle. However, significant uncertainty remains with respect to estimates of global fish biomass (Wilson et al., 2009; Irigoien et al., 2014; Proud et al., 2017, 2018, 2019; Jennings and Collingridge, 2015; Bar-On et al., 2018; Bianchi et al., 2021). At present, most biomass models lack resolution of regional hotspots, and may overlook fish smaller than 10 g (Bianchi et al., 2021). Smaller fish are known to produce more ichthyocarbonate per unit mass than larger fish (Wilson et al., 2009; Perry et al., 2011; Ghilardi et al., 2023), consequently, inclusion of small fish biomass in global ichthyocarbonate production estimates will likely increase total production estimates. In addition, mesopelagic fish biomass is notoriously difficult to measure (Saba et al., 2021) and has been proposed to constitute up to 95 % of the biomass of all marine fish (Dornan et al., 2019; Irigoien et al., 2014; Proud et al., 2019); lack of data makes estimates of ichthyocarbonate production by mesopelagic fish difficult. Prior quantification of ichthyocarbonate production rate has been conducted on unfed fish held at ambient temperatures (Wilson et al., 2009; Perry et al., 2011; Ghilardi et al., 2023), which likely resulted in conservative estimates, although the contrary was recently suggested (Ghilardi et al., 2023). However, Ghilardi et al. (2023) lacked an account of early and rapid dissolution in the collection tanks and relied upon a link between metabolic rate and

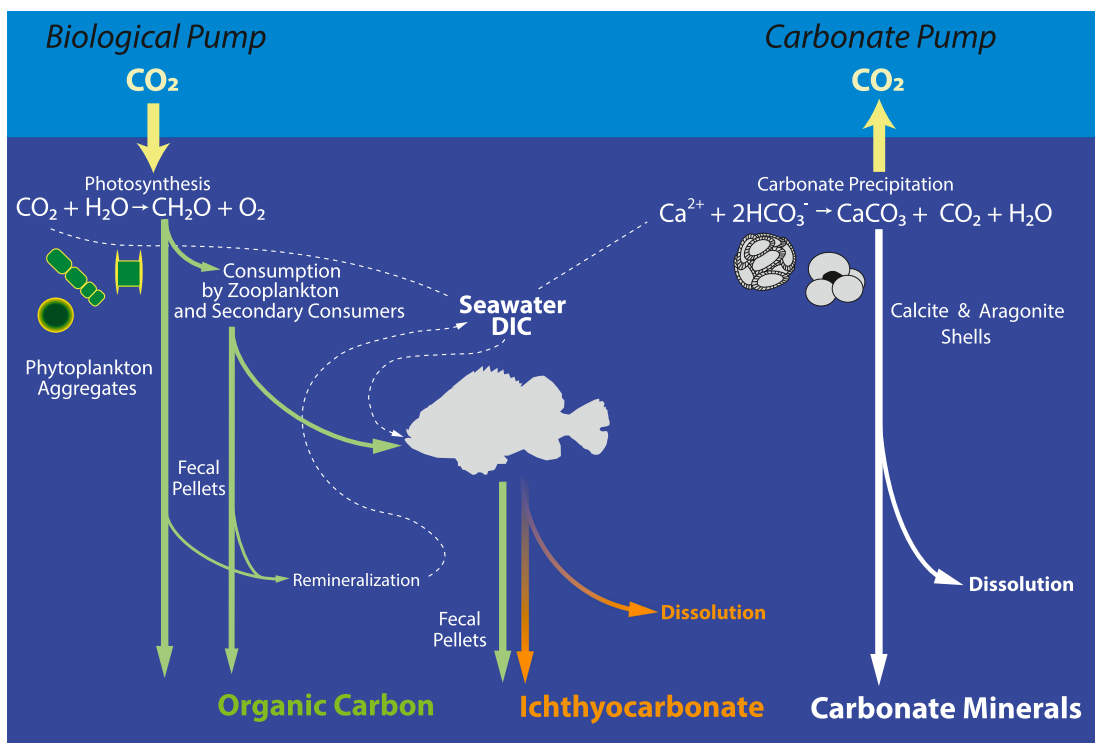


Fig. 6. Conceptual diagram illustrating how marine fish plausibly link the biological and carbonate pumps in the open ocean. Diagram shows impacts on atmospheric CO_2 (yellow arrows) produced by sinking fluxes of organic carbon (green arrows), ichthyocarbonate (orange arrow), and other marine carbonate minerals (white arrows). Ichthyocarbonate formation incorporates carbon both from seawater dissolved inorganic carbon and from the marine food web, linking ichthyocarbonate production to biogeochemical processes that draw down CO_2 .

relative intestinal length, rather than intestinal surface area, both of which could underestimate production rates. Future work should investigate a wider range of species, rates of ichthyocarbonate production by fed fish, the influence of lifestyle and temperature on production rates as well as fate of ichthyocarbonates upon release.

To evaluate C_{DIET} contributions to ichthyocarbonate, the IsoError mixing model (Phillips and Gregg, 2001) was used to calculate mean \pm 95 % confidence intervals (Fig. 3). Assumptions regarding the $\delta^{13}\text{C}_{\text{DIC}}$ values, and the fractionation associated with hydration/hydroxylation and mineral precipitation were necessarily made but informed by prior studies (Fig. 1; Sheppard and Schwarcz, 1970; DeNiro and Epstein, 1978; Romanek et al., 1992; McConaughay et al., 1997; Jimenez-Lopez et al., 2006; Swart et al., 2013). Future work should empirically define these fractionation factors to reduce uncertainty on these analyses. Results indicate a relatively high degree of variance in compositional characteristics of ichthyocarbonate produced by the species studied here (Table 2), thus, additional studies quantifying %TOC, PIC:POC ratios, % Carbonate, $\delta^{13}\text{C}_{\text{ichthyo}}$ and $\delta^{13}\text{C}_{\text{org}}$ in ichthyocarbonate produced by a wider variety of marine fish species are anticipated to improve constraints on global production. Despite the limitations of the current study, it is clear that marine fish make important contributions to carbonate production in the modern oceans.

5. Conclusions

Marine fish contribute a significant amount of carbonate to the oceans each year. Our estimates suggest global new carbonate production by marine fish ranges between 0.33 and 9.03 Pg $\text{CaCO}_3 \text{ yr}^{-1}$, potentially making fish one of the dominant carbonate producers in the sea. Results indicate that marine fish also utilize anomalously high concentrations of carbon derived from their diet (28–56 % on average) to precipitate ichthyocarbonate, compared to other producers which principally rely on dissolved inorganic carbon from seawater.

Considered within the potential global ichthyocarbonate production estimates calculated here, assessment of dietary carbon content in ichthyocarbonate suggests that between 0.09 and 5.05 Pg CaCO_3 produced each year may not conform to canonical expectations of the impact of carbonate production on the global carbon cycle. Because dietary carbon originates in the marine food web, from photosynthesis conducted by primary producers, the impacts of ichthyocarbonate production on seawater carbonate chemistry may not adhere to expectations regarding net CO_2 release, and future work should elucidate these impacts. Finally, ichthyocarbonate produced by two species was found to contain between 5.5 and 40.4 % TOC, present as an ichthyocarbonate-associated organic matrix. Scaled globally, this indicates a median production potential as high as 1.61 Pg C yr^{-1} , depending on global ichthyocarbonate production. Although fish physiologists have long been aware that dietary carbon must contribute to ichthyocarbonate production, connections between the physiology of ichthyocarbonate production and the biological pump have never previously been identified. Implications of ichthyocarbonate production rate and composition appear to position marine fish as a central component of Earth's global carbon cycle over the past \sim 300 million years.

CRediT authorship contribution statement

Amanda M. Oehlert: Writing – review & editing, Writing – original draft, Visualization, Methodology, Investigation, Funding acquisition, Formal analysis, Data curation, Conceptualization. **Jazmin Garza:** Investigation, Formal analysis, Data curation. **Sandy Nixon:** Investigation, Formal analysis, Data curation. **LeeAnn Frank:** Writing – review & editing, Writing – original draft, Visualization, Methodology, Investigation, Formal analysis, Data curation. **Erik J. Folkerts:** Writing – review & editing, Investigation, Formal analysis, Data curation. **John D. Stieglitz:** Writing – review & editing, Methodology, Investigation, Formal analysis, Data curation. **Chaojin Lu:** Writing – review & editing,

Methodology, Formal analysis, Data curation. **Rachael M. Heuer**: Writing – review & editing, Visualization, Methodology, Data curation, Conceptualization. **Daniel D. Benetti**: Writing – review & editing, Resources, Methodology, Investigation. **Javier del Campo**: Writing – review & editing, Investigation, Conceptualization. **Fabian A. Gomez**: Writing – review & editing, Visualization, Investigation, Conceptualization. **Martin Grosell**: Writing – original draft, Resources, Methodology, Investigation, Funding acquisition, Formal analysis, Data curation, Conceptualization.

Declaration of competing interest

The authors declare that they have no known competing financial interests or personal relationships that could have appeared to influence the work reported in this paper.

Data availability

Synthesized data are available in the main text and supplementary materials. Results of geochemical analyses of diet, ichthyo-carbonate composition, and $\delta^{13}\text{C}_{\text{ichthyo}}$ and mol% MgCO_3 in days past feeding are available as open access Mendeley Datasets at DOI: [10.17632/shs7hbpdj.1](https://doi.org/10.17632/shs7hbpdj.1) with a CC BY 4.0 License.

Acknowledgments

The authors acknowledge Emily Osborne, Peter Swart, April Mann, and two anonymous reviewers for feedback on an earlier draft of this manuscript. The Stable Isotope Laboratory, including Peter Swart and Amel Saeid, is thanked for analytical support. Amy Feltz is acknowledged for collecting yellowtail snapper ichthyo-carbonate for TOC analysis. A.M.O. is grateful to Hilary Close for ocean carbon cycle discussions. M.G. is a Maytag Chair of Ichthyology. The authors also acknowledge Open Blue Sea Farms for providing support to D.D.B. for an ongoing research agreement for the cobia program at UMEH. Finally, we thank three anonymous reviewers for feedback that improved this manuscript.

Funding

A.M.O. and M.G. are supported by the National Science Foundation (NSF-OCE-2319245). A.M.O. and J.d.C. acknowledge start-up funds provided by the Rosenstiel School of Marine, Atmospheric, and Earth Science at the University of Miami. E.J.F. is supported by a postdoctoral fellowship from the National Research Council of Canada, and C.L. is supported by the Stable Isotope Laboratory at the University of Miami's Rosenstiel School of Marine, Atmospheric, and Earth Science.

Appendix A. Supplementary data

Supplementary data to this article can be found online at <https://doi.org/10.1016/j.scitotenv.2024.169895>.

References

Armstrong, R.A., Lee, C., Hedges, J.I., Honjo, S., Wakeham, S.G., 2002. A new, mechanistic model for organic carbon fluxes in the ocean based on the quantitative association of POC with ballast minerals. *Deep-Sea Res. Pt II* **49**, 219–236.

Bar-On, Y.M., Phillips, R., Milo, R., 2018, Jun 19. The biomass distribution on earth. *Proc. Natl. Acad. Sci. U. S. A.* **115** (25), 6506–6511. <https://doi.org/10.1073/pnas.1711842115>.

Benetti, D.D., Orhun, M.R., Sardenberg, B., O'Hanlon, B., Welch, A., Hoenig, R., Zink, I., Rivera, J.A., Denlinger, B., Bacoat, D., Palmer, K., Cavalin, F., 2008a. Advances in hatchery and grow-out technology of cobia *Rachycentron canadum* (Linnaeus). *Aquac. Res.* **39** (7), 701–711.

Benetti, D.D., Sardenberg, B., Welch, A., Hoenig, R., Orhun, M.R., Zink, I., 2008b. Intensive larval husbandry and fingerling production of cobia *Rachycentron canadum*. *Aquaculture* **281**, 22–27.

Benetti, D.D., O'Hanlon, B., Rivera, J.A., Welch, A.W., Maxey, C., Orhun, M.R., 2010. Growth rates of cobia (*Rachycentron canadum*) in open ocean cages in the Caribbean. *Aquaculture* **302**, 195–201.

Benetti, D.D., Suarez, J., Camperio, J., Hoenig, R.H., Tudela, C.E., Daugherty, Z., McGuigan, C.J., Mathur, S., Ancheta, L., Buchalla, Y., Alarcón, J., Marchetti, D., Fiorentino, J., Buchanan, J., Artiles, A., Stieglitz, J.D., 2021. A review on cobia, *Rachycentron canadum*, aquaculture. Review article. *J. World Aquacult. Soc.* **2021**, 1–19. <https://doi.org/10.1111/jwas.12810>.

Bianchi, D., Carozza, D., Galbraith, E., Guiet, J., DeVries, T., 2021. Estimating global biomass and biogeochemical cycling of marine fish with and without fishing. *Sci. Adv.* **7**, eabd7554.

Boyd, P.W., Claustre, H., Levy, M., Siegel, D.A., Weber, T., 2019, Apr. Multi-faceted particle pumps drive carbon sequestration in the ocean. *Nature* **568** (7752), 327–335. <https://doi.org/10.1038/s41586-019-1098-2>.

Broecker, W., Clark, E., 2009. Ratio of coccolith CaCO_3 to foraminifera CaCO_3 in late Holocene deep sea sediments. *Paleoceanography* **24** (3). <https://doi.org/10.1029/2009pa001731>.

Buesseler, K.O., Boyd, P.W., Black, E.E., Siegel, D.A., 2020, May 5. Metrics that matter for assessing the ocean biological carbon pump. *Proc. Natl. Acad. Sci. U. S. A.* **117** (18), 9679–9687. <https://doi.org/10.1073/pnas.1918114117>.

Buitenhuis, E.T., Le Quere, C., Bednarsek, N., Schiebel, R., 2019, Mar. Large contribution of pteropods to shallow CaCO_3 export. *Glob. Biogeochem. Cycles* **33** (3), 458–468. <https://doi.org/10.1029/2018GB006516>.

Chung, M.T., Jørgensen, K.E.M., Trueman, C.N., Knutson, H., Jorde, P.E., Grønkjær, P., 2020. First measurements of field metabolic rate in wild juvenile fishes show strong thermal sensitivity but variations between sympatric ecotypes. *Oikos* **130** (2), 287–299. <https://doi.org/10.1111/oik.07647>.

Chung, M.-T., Trueman, C.N., Godiksen, J.A., Grønkjær, P., 2019. Otolith $\delta^{13}\text{C}$ values as a metabolic proxy: approaches and mechanical underpinnings. *Mar. Freshw. Res.* **70** (12) <https://doi.org/10.1071/mf18317>.

Coplen, T.B., Brand, W.A., Gehre, M., Gröning, M., Meijer, H.A.J., Toman, B., Verkouteren, R.M., 2006. New guidelines for $\delta^{13}\text{C}$ measurements. *Anal. Chem.* **78**, 2439–2441.

DeNiro, M.J., Epstein, S., 1978. Influence of diet on the distribution of carbon isotopes in animals. *Geochem. Cosmochim. Acta* **42**, 495–506.

DeVries, T., 2022. The Ocean Carbon Cycle. *Annu. Rev. Environ. Resour.* **47**, 317–341.

Dornan, T.J., Fielding, S., Saunders, R.A., Genner, M.J., 2019, May 29. Swimbladder morphology masks Southern Ocean mesopelagic fish biomass. *Proc. Biol. Sci.* **286** (1903), 20190353. <https://doi.org/10.1098/rspb.2019.0353>.

Elderfield, H., 2002. Carbonate mysteries. *Science* **296**, 1618–1621.

Findlay, H., Calosi, P., Crawford, K., 2011. Determinants of the PIC:POC response in the coccolithophore *Emiliania huxleyi* under future ocean acidification scenarios. *Limnol. Oceanogr.* **56** (3), 1168–1178.

Foran, E., Weiner, S., Fine, M., 2013. Biogenic fish-gut calcium carbonate is a stable amorphous phase in the gilt-head seabream, *Sparus aurata*. *Sci. Rep.* **3**, 1700. <https://doi.org/10.1038/srep01700>.

Frankignoulle, M., Canon, C., Gattuso, J.-P., 1994. Marine calcification as a source of carbon dioxide: positive feedback of increasing atmospheric CO_2 . *Limnol. Oceanogr.* **39** (2), 458–462. <https://doi.org/10.4319/lo.1994.39.2.0458>.

Frankignoulle, M., Pichon, M., Gattuso, J.-P., 1995. Aquatic calcification as a source of carbon dioxide. In: *Carbon Sequestration in the Biosphere*, pp. 265–271. https://doi.org/10.1007/978-3-642-79943-3_18.

Gattuso, J.P., Pichon, M., Delesalle, B., Frankignoulle, M., 1993. Community metabolism and air-sea CO_2 fluxes in a coral reef ecosystem (Moorea, French Polynesia). *Mar. Ecol. Prog. Ser.* **95**, 259–267.

Geng, J., Belfranin, C., Zander, I.A., Goldstein, E., Mathur, S., Lederer, B.I., Benvenuti, R., Benetti, D., 2017. Effect of stocking density and feeding regime on larval growth, survival, and larval development of Japanese flounder, *Paralichthys olivaceus*, using live feeds. *J. World Aquacult. Soc.* **2018**, 1–10. <https://doi.org/10.1111/jwas.12563>.

Genz, J., Esbbaugh, A.J., Grosell, M., 2011. Intestinal transport following transfer to increased salinity in an anadromous fish (*Oncorhynchus mykiss*). *Comp. Biochem. Physiol. A Mol. Integr. Physiol.* **159** (2), 150–158.

Genz, J., Taylor, J.R., Grosell, M., 2008, Jul 15. Effects of salinity on intestinal bicarbonate secretion and compensatory regulation of acid-base balance in *Opsanus beta*. *J. Exp. Biol.* **211** (14), 2327–2335. <https://doi.org/10.1242/jeb.016832>.

Ghilardi, M., Salter, M.A., Parravicini, V., Ferse, S.C.A., Rixen, T., Wild, C., Birkicht, M., Perry, C.T., Berry, A., Wilson, R.W., Mouillet, D., Bejarano, S., 2023. Temperature, species identity and morphological traits predict carbonate excretion and mineralogy in tropical reef fishes. *Nat. Commun.* **14** (1), 985. <https://doi.org/10.1038/s41467-023-36617-7>.

Gloege, L., McKinley, G.A., Mouw, C.B., Ciochetto, A.B., 2017. Global evaluation of particulate organic carbon flux parameterizations and implications for atmospheric pCO_2 . *Glob. Biogeochem. Cycles* **31** (7), 1192–1215. <https://doi.org/10.1002/2016gb005535>.

Godrijan, J., Drapeau, D.T., Balch, W.M., 2022. Osmotrophy of dissolved organic carbon by coccolithophores in darkness. *New Phytol.* **233** (2), 781–794. <https://doi.org/10.1111/nph.17819>.

Goldsmith, J.R., Graf, D.L., Heard, H.C., 1961. Lattice constants of the calcium-magnesium carbonates. *Am. Mineral.* **46**, 453–459.

Grosell, M., 2010. The role of the gastrointestinal tract in salt and water balance. In: Grosell, Martin, Farrell, Anthony P., Brauner, Colin J. (Eds.), *Fish Physiology, The Multifunctional Gut of Fish*, 30, pp. 135–164.

Grosell, M., Oehlert, A.M., 2023. Staying hydrated in seawater. *Physiology* **38**, 1–11.

Grosell, M., Genz, J., 2006. Ouabain sensitive bicarbonate secretion and acid adsorption by the marine fish intestine play a role in osmoregulation. *Am. J. Physiol.* 291, R1145–R1156.

Grosell, M., Laliberte, C.N., Wood, S., Jensen, F.B., Wood, C.M., 2001. Intestinal HCO_3^- secretion in marine teleost fish: evidence for an apical rather than a basolateral Cl_- / HCO_3^- exchanger. *Fish Physiol. Biochem.* 24 (2), 81–95.

Grossman, E.L., Betzer, P.R., Dudley, W.C., Dunbar, R.B., 1986. Stable isotopic variation in pteropods and atlantids from North Pacific sediment traps. *Mar. Micropaleontol.* 10 (1–3), 9–22.

Heuer, R.M., Eshaugh, A.J., Grosell, M., 2012. Ocean acidification leads to counterproductive intestinal base loss in the gulf toadfish (*Opsanus Beta*). *Physiol. Biochem. Zool.* 85 (5), 450–459. <https://doi.org/10.1086/667617>, 9/2012.

Heuer, R.M., Munley, K.M., Narsanghai, N., Wingar, J.A., Mackey, T., Grosell, M., 2016. Changes to intestinal transport physiology and carbonate production at various CO_2 levels in a marine teleost, the Gulf toadfish (*Opsanus beta*). *Physiol. Biochem. Zool.* 89 (5), 402–416.

Honjo, S., Eglington, T., Taylor, C., Ulmer, K., Sievert, S., Bracher, A., German, C., Edgcomb, V., Francois, R., Iglesias-Rodriguez, M.D., Van Mooy, B., Rapeta, D., 2014. Understanding the role of the biological pump in the global carbon cycle: an imperative for ocean science. *Oceanography* 27 (3), 10–16. <https://doi.org/10.5670/oceanog.2014.78>.

Hopkins, J.B., Ferguson, J.M., 2012. Estimating the diets of animals using stable isotopes and a comprehensive Bayesian mixing model. *PLoS One* 7 (1), e28478.

Iglesias-Rodriguez, M.D., Armstrong, R.A., Feely, R.A., Hood, R., Kleypas, J., Milliman, J. D., Sabine, C.L., Sarmiento, J.L., 2002. Progress made in study of ocean's calcium carbonate budget. *Eos* 83 (34).

Irigoién, X., Klevjer, T.A., Rostad, A., Martínez, U., Boyra, G., Acuna, J.L., Bode, A., Echevarría, F., González-Gordillo, J.I., Hernández-León, S., Agustí, S., Aksnes, D.L., Duarte, C.M., Kaartvedt, S., 2014. Large mesopelagic fishes biomass and trophic efficiency in the open ocean. *Nat. Commun.* 5, 3271. <https://doi.org/10.1038/ncomms4271>.

Jennings, S., Collingridge, K., 2015. Predicting consumer biomass, size-structure, production, catch potential, responses to fishing and associated uncertainties in the world's marine ecosystems. *PLoS One* 10 (7), e0133794. <https://doi.org/10.1371/journal.pone.0133794>.

Jimenez-Lopez, C., Romanek, C.S., Caballero, E., 2006. Carbon isotope fractionation in synthetic magnesian calcite. *Geochim. Cosmochim. Acta* 70 (5), 1163–1171. <https://doi.org/10.1016/j.gca.2005.11.005>.

Jobling, M., 1981. The influences of feeding on the metabolic-rate of fishes - a short review. *J. Fish Biol.* 18 (4), 385–400. <https://doi.org/10.1111/j.1095-8649.1981.tb03780.x>.

Jobling, M., Davies, P.S., 1980. Effects of feeding on metabolic rate, and the specific dynamic action in plaice, *Pleuronectes platessa* L. *J. Fish Biol.* 16 (6), 629–638. <https://doi.org/10.1111/j.1095-8649.1980.tb03742.x>.

Klaas, C., Archer, D.E., 2002. Association of sinking organic matter with various types of mineral ballast in the deep sea: implications for the rain ratio. *Glob. Biogeochem. Cycles* 16 (4). <https://doi.org/10.1029/2001gb001765>, 63–61–63–14.

Langer, M.R., 2008. Assessing the contribution of foraminiferal protists to global ocean carbonate production. *Eukaryotic Microbiol.* 55 (3), 163–169.

Mariani, G., Cheung, W.W.L., Lyet, A., Sala, E., Mayorga, J., Velez, L., Gaines, S.D., Dejean, T., Troussellier, M., Moullot, D., 2020. Let more big fish sink: fisheries prevent blue carbon sequestration-half in unprofitable areas. *Sci. Adv.* 6, eabb4848.

McConaughey, T.A., 1989. ^{13}C and ^{18}O isotopic disequilibrium in biological carbonates: I. Patterns. *Geochim. Cosmochim. Acta* 53 (1), 151–162.

McConaughey, T.A., Burdett, J., Whelan, J.F., Paull, C.K., 1997. Carbon isotopes in biological carbonates: respiration and photosynthesis. *Geochim. Cosmochim. Acta* 61 (3), 611–622.

McDonald, M.D., Grosell, M., 2006. Maintaining osmotic balance with an agglomerular kidney. *Comp. Biochem. Physiol. Part A Mol. Integr. Physiol.* 143 (4), 447–458, 4/2006.

Milliman, J.D., Droxler, A.W., 1996. Neritic and pelagic carbonate sedimentation in the marine environment: ignorance is not bliss. *Geol. Rundsch.* 85, 496–504.

Nowicki, M., DeVries, T., Siegel, D.A., 2022. Quantifying the carbon export and sequestration pathways of the ocean's biological carbon pump. *Glob. Biogeochem. Cycles* 36 (3). <https://doi.org/10.1029/2021gb007083>.

Oehlert, A.M., Swart, P.K., 2014. Interpreting carbonate and organic carbon isotope covariance in the sedimentary record. *Nat. Commun.* 5, 4672. <https://doi.org/10.1038/ncomms5672>.

Perry, C.T., Salter, M.A., Harborne, A.R., Crowley, S.F., Jelks, H.L., Wilson, R.W., 2011. Fish as major carbonate mud producers and missing components of the tropical carbonate factory. *Proc. Natl. Acad. Sci. U. S. A.* 108 (10), 3865–3869. <https://doi.org/10.1073/pnas.1015895108>.

Perry, C.T., Salter, M.A., Lange, I.D., Kochan, D.P., Harborne, A.R., Graham, N.A.J., 2022. Geo-ecological functions provided by coral reef fishes vary among regions and impact reef carbonate cycling regimes. *Ecosphere* 13 (12). <https://doi.org/10.1002/ecs2.4288>.

Perry, S.F., Braun, M.H., Genz, J., Vulesevic, B., Taylor, J., Grosell, M., Gilmour, K.M., 2010. Acid-base regulation in the plainfin midshipman (*Porichthys notatus*): an agglomerular marine teleost. *J. Comp. Physiol. B* 180 (8), 1213–1225. <https://doi.org/10.1007/s00360-010-0492-8>.

Phillips, D.L., Gregg, J.W., 2001. Uncertainty in source partitioning using stable isotopes. *Oecologia* 127, 171–179.

Pinti, J., DeVries, T., Norin, T., Serra-Pompeii, C., Proud, R., Siegel, D.A., Kiorboe, T., Petrik, C.M., Andersen, K.H., Brierley, A.S., Visser, A.W., 2023. Model estimates of metazoans' contributions to the biological carbon pump. *Biogeosciences* 20 (5), 997–1009. <https://doi.org/10.5194/bg-20-997-2023>.

Proud, R., Cox, M.J., Brierley, A.S., 2017. Biogeography of the global ocean's mesopelagic zone. *Curr. Biol.* 27 (1), 113–119.

Proud, R., Cox, M.J., Le Guen, C., Brierley, A.S., 2018. Fine-scale depth structure of pelagic communities throughout the global ocean based on acoustic sound scattering layers. *Mar. Ecol. Prog. Ser.* 598, 35–48.

Proud, R., Handegard, N.O., Kloser, R.J., Cox, M.J., Brierley, A.S., Demer, D., 2019. From siphonophores to deep scattering layers: uncertainty ranges for the estimation of global mesopelagic fish biomass. *ICES J. Mar. Sci.* 76 (3), 718–733. <https://doi.org/10.1093/icesjms/fsy037>.

Romanek, C.S., Grossman, E.L., Morse, J.W., 1992. Carbon isotopic fractionation in synthetic aragonite and calcite: effects of temperature and precipitation rate. *Geochim. Cosmochim. Acta* 56 (1), 419–430.

Rosenheim, B.E., Swart, P.K., Thorrold, S.R., Eisenhauer, A., 2005. Salinity change in the subtropical Atlantic: secular increase and teleconnections to the North Atlantic oscillation. *Geophys. Res. Lett.* 32 (2). <https://doi.org/10.1029/2004gl021499>.

Saba, G.K., Steinberg, D.K., 2012. Abundance, composition, and sinking rates of fish fecal pellets in the Santa Barbara Channel. *Sci. Rep.* 2, 716. <https://doi.org/10.1038/srep00716>.

Saba, G.K., Burd, A.B., Dunne, J.P., Hernández-León, S., Martin, A.H., Rose, K.A., Salisbury, J., Steinberg, D.K., Trueman, C.N., Wilson, R.W., Wilson, S.E., 2021. Toward a better understanding of fish-based contribution to ocean carbon flux. *Limnol. Oceanogr.* <https://doi.org/10.1002/lno.11709>.

Salter, M.A., 2013. The Production and Preservation of Fish-derived Carbonates in Shallow Sub-tropical Marine Carbonate Provinces. *Manchester Metropolitan University*.

Salter, M.A., Perry, C.T., Wilson, R.W., 2012. Production of mud-grade carbonates by marine fish: crystalline products and their sedimentary significance. *Sedimentology* 59 (7), 1–27.

Salter, M.A., Perry, C.T., Wilson, R.W., 2014. Size fraction analysis of fish-derived carbonates in shallow sub-tropical marine environments and a potentially unrecognised origin for peloidal carbonates. *Sediment. Geol.* 314, 17–30.

Salter, M.A., Harborne, A.R., Perry, C.T., Wilson, R.W., 2017. Phase heterogeneity in carbonate production by marine fish influences their roles in sediment generation and the inorganic carbon cycle. *Sci. Rep.* 7 (1), 765. <https://doi.org/10.1038/s41598-017-00787-4>.

Salter, M.A., Perry, C.T., Stuart-Smith, R.D., Edgar, G.J., Wilson, R.W., Harborne, A.R., 2018. Reef fish carbonate production assessments highlight regional variation in sedimentary significance. *Geology* 46 (8), 699–702. <https://doi.org/10.1130/g45286.1>.

Salter, M.A., Perry, C.T., Smith, A.M., 2019. Calcium carbonate production by fish in temperate marine environments. *Limnol. Oceanogr.* 64 (6), 2755–2770. <https://doi.org/10.1002/lno.11339>.

Schaffer, R.V., Nakamura, E.L., 1989. Synopsis of biological data on the Cobia *Rachycentron canadum* (Pisces: Rachycentridae). In: NOAA Technical Report NMFS 82, FAO Fisheries Synopsis, 153, pp. 1–18.

Schauer, K.L., Grosell, M., 2017. Jun. Fractionation of the gulf toadfish intestinal precipitate organic matrix reveals potential functions of individual proteins. *Comp. Biochem. Physiol. Part A Mol. Integr. Physiol.* 208, 35–45.

Schauer, K.L., LeMoine, C.M.R., Pelin, A., Corradi, N., Warren, W.C., Grosell, M., 2016. A proteinaceous organic matrix regulates carbonate mineral production in the marine teleost intestine. *Sci. Rep.* 6 (1), 34494.

Schauer, K.L., Christensen, E.A.F., Grosell, M., 2018a. Comparison of the organic matrix found in intestinal CaCO_3 precipitates produced by several marine teleost species. *Comp. Biochem. Physiol. Part A Mol. Integr. Physiol.* 221, 15–23.

Schauer, K.L., Reddam, A., Xu, E.G., Wolfe, L.M., Grosell, M., 2018b. Interrogation of the Gulf toadfish intestinal proteome response to hypersalinity exposure provides insight into osmoregulatory mechanisms and regulation of carbonate mineral precipitation. *Comp. Biochem. Physiol. D* 27, 66–76.

Shehadeh, Z.H., Gordon, M.S., 1969. The role of the intestine in salinity adaptation of the rainbow trout, *Salmo gairdneri*. *Comp. Biochem. Physiol.* 30, 397–418.

Sheppard, S.M.F., Schwarzh, H.P., 1970. Fractionation of carbon and oxygen isotopes and magnesium between coexisting metamorphic calcite and dolomite. *Contrib. Mineral. Petro.* 26 (3), 161–198.

Spero, H.J., Lea, D.W., 1996. Experimental determination of stable isotope variability in *Globigerina bulloides*: implications for paleoceanographic reconstructions. *Mar. Micropaleontol.* 28, 231–246.

Staresinic, N., Farrington, J., Gagopian, R.B., Clifford, C.H., Hulbert, E.M., 1983. Downward transport of particulate matter in the Peru coastal upwelling: role of the Anchoveta, Engraulis Ringens. In: *Coastal Upwelling Its Sediment Record*, pp. 225–240. https://doi.org/10.1007/978-1-4615-6651-9_12.

Stieglitz, J., Benetti, D., Hoenig, R., Sardenberg, B., Welch, A., Miralao, S., 2012. Environmentally conditioned, year-round volitional spawning of cobia (*Rachycentron canadum*) in broodstock maturation systems. *Aquac. Res.* 43, 1557–1566.

Stieglitz, J., Hoenig, R., Baggett, J., Tudela, C., Mathur, S., Benetti, D., 2021. Advancing production of marine fish in the U.S.: olive flounder, *Paralichthys olivaceus*, aquaculture. *J. World Aquacult. Soc.* 52 (3), 566–581. <https://doi.org/10.1111/jwas.12804>.

Swart, P.K., Anderson, W.T., Altabet, M.A., Drayer, C., Bellmund, S., 2013. Sources of dissolved inorganic nitrogen in a coastal lagoon adjacent to a major metropolitan area, Miami Florida (USA). *Appl. Geochem.* 38, 134–146. <https://doi.org/10.1016/j.apgeochem.2013.09.008>.

Turner, J.T., 2015. Zooplankton fecal pellets, marine snow, phydetritus and the ocean's biological pump. *Prog. Oceanogr.* 130, 205–248. <https://doi.org/10.1016/j.pocean.2014.08.005>.

Urban, J.L., Deibel, D., Schwinghamer, P., 1993. Seasonal variations in the densities of fecal pellets produced by *Oikopleura vanhoeffeni* (C. Larvacea) and *Calanus finmarchicus* (C. Copepoda). *Mar. Biol.* 117, 607–613.

Walsh, P., Blackwelder, P., Gill, K., Danulat, E., MommSEN, T., 1991. Carbonate deposits in marine fish intestines: a new source of biomineralization. *Limnol. Oceanogr.* 36, 1227–1232.

Ware, J.R., Smith, S.V., Reaka-Kudla, M.L., 1991. Coral reefs: sources of sinks of atmospheric CO₂? *Coral Reefs* 11, 127–130.

Weber, T., Cram, J.A., Leung, S.W., DeVries, T., Deutsch, C., 2016, Aug 2. Deep ocean nutrients imply large latitudinal variation in particle transfer efficiency. *Proc. Natl. Acad. Sci. U. S. A.* 113 (31), 8606–8611. <https://doi.org/10.1073/pnas.1604414113>.

White, M.M., Waller, J.D., Lubelczyk, L.C., Drapeau, D.T., Bowler, B.C., Balch, W.M., Fields, D.M., 2018. Coccolith dissolution within copepod guts affects fecal pellet density and sinking rate. *Sci. Rep.* 8, 1–6.

Wilson, R.W., Gilmour, K., Henry, R., Wood, C., 1996a. Intestinal base excretion in the seawater-adapted rainbow trout: a role in acid-base balance? *J. Exp. Biol.* 199 (Pt 10), 2331–2343. <http://www.ncbi.nlm.nih.gov/pubmed/9320250>.

Wilson, R.W., Gilmour, K.M., Henry, R.P., Wood, C.M., 1996, Oct. Intestinal base excretion in the seawater-adapted rainbow trout: a role in acid-base balance? *J. Exp. Biol.* 199 (10), 2331–2343.

Wilson, R.W., Wilson, J.M., Grosell, M., 2002. Intestinal bicarbonate secretion by marine teleost fish—why and how? *Biochim. Biophys. Acta* 1566 (1–2), 182–193. <http://www.ncbi.nlm.nih.gov/pubmed/12421549> (Not in File).

Wilson, R.W., Millero, F.J., Taylor, J.R., Walsh, P.J., Christensen, V., Jennings, S., Grosell, M., 2009, Jan 16. Contribution of fish to the marine inorganic carbon cycle. *Science* 323 (5912), 359–362.

Woosley, R.J., Millero, F.J., Grosell, M., 2012. The solubility of fish-produced high magnesium calcite in seawater. *J. Geophys. Res. Oceans* 117 (C4). <https://doi.org/10.1029/2011jc007599> n/a-n/a.

Zeebe, R.E., Wolf-Gladrow, D.A., 2001. CO₂ in Seawater: Equilibrium, Kinetics, Isotopes. Elsevier.